Available online at www.sciencedirect.com
ScienceDirect
The International Journal of Biochemistry & Cell Biology 40 (2008) 1918–1929
IJBCB
www.elsevier.com/locate/biocel

Anticancer effects of ginsenoside Rg1, cinnamic acid, and tanshinone IIA in osteosarcoma MG-63 cells: Nuclear matrix downregulation and cytoplasmic trafficking of nucleophosmin

Qi-Fu Li [a,*], Song-Lin Shi [a], Qing-Rong Liu [b], Jian Tang [a], Jianye Song [a], Ying Liang [a]

[a] *Key Laboratory of Ministry of Education for Cell Biology & Tumor cell Engineering, School of Life Sciences, Xiamen University, Xiamen 361005, PR China*

[b] *Molecular Neurobiology Branch, National Institute on Drug Abuse-Intramural Research Program (NIDA-IRP), NIH, Department of Health and Human Services (DHSS), 333 Cassell Drive, Baltimore, MD 21224, USA*

Received 29 November 2007; received in revised form 28 January 2008; accepted 29 January 2008
Available online 12 February 2008

Abstract

Ginsenoside Rg1, cinnamic acid, and tanshinone IIA are effective anticancer and antioxidant constituents of traditional Chinese herbal medicines of Ginseng (*Panax ginseng*), Xuanshen (*Radix scrophulariae*), and Danshen (*Salvia mitiorrhiza*), respectively. There was insufficient study on molecular mechanisms of anticancer effects of those constituents and their targets were unknown. We chose nucleophosmin as a candidate molecular target because it is frequently mutated and upregulated in various cancer cells. Nucleophosmin is a major nucleolus phosphoprotein that involves in rRNA synthesis, maintaining genomic stability, and normal cell division and its haploinsufficiency makes cell more susceptible to oncogenic assault. Ginsenoside Rg1, cinnamic acid, and tanshinone IIA treatment of osteosarcoma MG-63 cells decreased nucleophosmin expression in nuclear matrix and induced nucleophosmin translocation from nucleolus to nucleoplasm and cytoplasm, a process of dedifferentiating transformed cells. Using immunogold electro-microscopy, we found at the first time that nucleophosmin was localized on nuclear matrix intermediate filaments that had undergone restorational changes after the treatments. Nucleophosmin also functions as a molecular chaperone that might interact with multiple oncogenes and tumor suppressor genes. We found that oncogenes c-myc, c-fos and tumor suppressor genes, P53, Rb were regulated by ginsenoside Rg1, cinnamic acid, and tanshinone IIA as well. In present study, we identified nucleophosmin as a molecular target of the effective anticancer constituents of t Ginseng, Xuanseng, and Danseng that down-regulated nucleophosmin in nuclear matrix, changed its trafficking from nucleolus to cytoplasm, and regulated several oncogenes and tumor suppressor genes. Therefore, we postulate that Ginsenoside Rg1, cinnamic acid, and tanshinone IIA could serve as protective agents in cancer prevention and treatment.

Keywords: Ginsenoside; Nucleophosmin; Human osteosarcoma; Nuclear matrix; Induced differentiation

1. Introduction

Ginseng (*Panax ginseng*), Xuanshen (*Radix scrophulariae*), and Danshen (*Salvia mitiorrhiza*) literately mean in Chinese "essences of the earth in the form of a man, a saint, and a cardinal", respectively. They were highly

* Corresponding author. Tel.: +86 592 2185363; fax: +86 592 2181015.
E-mail address: chifulee@xmu.edu.cn (Q.-F. Li).

1357-2725/$ – see front matter © 2008 Elsevier Ltd. All rights reserved.
doi:10.1016/j.biocel.2008.01.031

treasured in Chinese traditional medicines for maintaining youth, promoting longevity, and balancing whole body ying and yang to prevent diseases. Ginsenoside Rg1, cinnamic acid, and tanshinone IIA (RCT) are effective constituents of Ginseng, Xuanshen, and Danshen, respectively. Previous studies showed that RCT prevent tumor growth through reversal of gene expression of transformed cells by antioxidant, anti-inflammatory and apoptotic mechanisms (Helms, 2004; Yun, 2001). However, RCT treatment of cancer is controversial because their adverse interactions with other anticancer drugs (Sparreboom, Cox, Acharya, & Figg, 2004). The molecular mechanisms of RCT anticancer effects were not well understood. We previously found that osteosarcoma MG-63 cells could be induced to differentiation by RCT. In this study, we used osteosarcoma MG-63 cells as a model to investigated RCT effect on a major nucleolus phosphoprotein, nucleophosmin (NPM), whose trafficking from nucleolus to nucleoplasm and cytoplasm was used to test effectiveness of anticancer drugs (Chan, Qi, Amley, & Koller, 1996; Yung, 2007; Yung, Yang, & Bor, 1991).

Nucleophosmin plays multiple roles in tumorogenesis by functions in rRNA processing (Savkur & Olson, 1998), histone chaperone (Okuwaki, Matsumoto, Tsujimoto, & Nagata, 2001; Szebeni & Olson, 1999), centrosome duplication (Okuda et al., 2000), negative regulation of the ARF-P53 tumor suppressor pathway (Colombo, Marine, Danovi, Falini, & Pelicci, 2002; Colombo et al., 2005; Li, Zhang, Sejas, & Pang, 2005). NPM mutations were frequently observed in acute myologenous leukemia with normal karyotype (AML-NK) and NPM cytoplasmic location in leukemic blasts forming a prognostically favorable subgroups to induction of chemotherapy (Falini et al., 2005; Falini, Nicoletti, Martelli, & Mecucci, 2007). Chromosomal translocations at NPM gene locus were found in anaplastic lymphoma with t(2;5)(p23;q35) (Morris et al., 1994), acute promyelocytic leukemia t(5;17)(q35;q12) (Redner, 2002), and acute myeloid leukemia t(3;5)(q25;q35) (Raimondi et al., 1989). NPM homozygous knockout mice were embryonic lethal and heterozygous knockout mice were NPM gene haploinsufficient with increased susceptibility to oncogenic transformation (Grisendi et al., 2005). NPM is tightly bond to nuclear matrix in association with induction of proliferation in lymphocytes (Feuerstein & Mond, 1987; Feuerstein, Spiegel, & Mond, 1988) and localized in nuclear matrix intermediate filament system in human hepatocarcinoma cells (Tang et al., 2007). In this study, we further explored differential expression and intermediate filament localization of nucleophosmin in the nuclear matrix during the differentiation of MG-63 cell induced by RCT.

2. Materials and methods

2.1. Cell culture and treatment

The osteosarcoma MG-63 cells, provided by China Center for Type Culture Collection (CCTCC), were maintained in RPMI-1640 medium supplemented with 15% heat-inactivated fetal calf serum, 100 U mL^{-1} penicillin, 100 $\mu g\,mL^{-1}$ streptomycin and 50 $\mu g\,mL^{-1}$ kanamycin at 37 °C, 5% CO_2 in air atmosphere. After being seeded for 24 h, MG-63 cells were treated with culture medium containing the combination of 33 $\mu g\,mL^{-1}$ ginsenoside Rg1, 0.3 $\mu g\,mL^{-1}$ cinnamic acid and 0.3 $\mu g\,mL^{-1}$ tanshinone IIA (shortened form RCT) for 7 days to induce differentiation. Meanwhile, MG-63 cells were cultured in RPMI-1640 medium as the control group. The components of RCT are the standards bought from National Institute of the Control for the Pharmaceutical and Biological Products (NCPBP). The concentration of RCT was decided by previous work which evaluated the effects of terminal differentiation on MG-63 cells treated with the components and the combination of RCT.

2.2. Extraction of nuclear matrix proteins (NMPs)

For 2-DE analysis, the extraction method used was modified from Fey and Nickerson et al. (Gao, Han, Jiao, & Zhai, 1994; Michishita et al., 2002; Nickerson, Krockmalnic, Wan, & Penman, 1997). Harvested MG-63 cells were firstly washed with ice-cold PBS twice and then extracted by cytoskeleton (CSK) buffer (100 mM KCl, 3 mM MgCl, 5 mM EGTA, 10 mM PIPES, pH 6.8, 300 mM sucrose, 0.5% Triton X-100, 2 mM PMSF) for 10 min at 0 °C. After being centrifuged at 600 × *g* for 5 min, the pellets were washed with ice-cold PBS to remove soluble cytoplasmic proteins. They were then re-centrifuged and suspended within digestion buffer (same as CSK buffer except with 50 mM NaCl instead of KCl) containing 400 mg mL^{-1} DNase I for 30 min at room temperature. Cold ammonium sulfate was added to a final concentration of 0.25 M to terminate the enzyme digestion. After centrifugation at 1000 × *g* for 10 min, the pellets were washed with CSK buffer and then dissovolved in lysis buffer (7 M urea, 2 M thiourea, 4% CHAPS, 1.5% Triton X-100, 1% Pharmalyte (pH 3–10, Amersham Biosciences), 65 mM DTT, 40 mM Tris, 5 mg/mL aprotinin, 1 mg/mL leupeptin, 1 mg/mL pepstatin, and 2 mM PMSF, 5 mM EDTA). The sam-

ple was sonicated at 0 °C for 30 min and centrifuged at 15,000 × *g* for 1 h. The protein concentrations of the control and treated supernatants were determined by the Bradford assay, and then diluted to the same concentration (about 5 mg/mL) with lysis buffer and stored at −70 °C until future use.

2.3. Two-dimensional gel electrophoresis and image analysis

2D PAGE was performed with general methods. The gels were stained with silver nitrate protocol compatible with MS. Image scanning (UMAX PowerLook III) and analysis (PDQuest 8.0 software, Bio-Rad) for the three repeat sets silver-stained 2D gels were performed. After the background subtraction, spot detection and match, spot intensities were obtained by integration of the Gaussian function with unit of intensity calculated as "Intensity × Area as parts per million" (INT × area PPM). The intensity of each protein spot was normalized to the total intensity of the entire gel. The spots of protein whose intensity changed twofold were defined as differentially expressed NMPs.

2.4. MALDI-TOF-MS analysis and protein identification

The spots of differentially expressed proteins were cut out from the gels. After a series of steps including silver removal, reduction with DL-dithiothreitol, alkylation with iodacetamide, and in-gel digestion with trypsin, the peptide mass finger (PMF) maps were generated by Bruke III MALDI-TOF mass spectrometry. Flex Analysis software was used to analyze the PMF data so as to calibrate and remove polluted peaks. The data were then searched against NCBInr and Swiss-Prot protein databases using Mascot tool from Matrix Science.

2.5. Western blot

The nuclear matrix proteins were separated by SDS-PAGE and then transferred onto PVDF membranes. Nonspecific reactivity was blocked by incubation at 4 °C for 1 h in 4%BSA buffer. The membrane was then incubated with NPM primary antibody at room temperature for 3 h. After being washed, the secondary antibody (combined with horseradish peroxidase) was used to detect bound primary antibody. Reactive protein was detected by enhanced chemiluminescence (ECL) detection system (Pierce). The quantitative analysis of each protein band was performed by gel analysis software Quantity One (Bio-Rad).

2.6. Sample preparation for NM-IF system

The cells were selectively extracted as described below (Capco, Wan, & Penman, 1982). The cells treated with or without RCT were seeded in small bottles with cover slip strip on which there were some nickel grids covered with formvar, coated with carbon, and covered with polylysine. The cells were rinsed with D-Hank's solution twice at 37 °C, and extracted by high-ionic strength extraction solution (10 mmol L^{-1} PIPES, pH 6.8, 250 mmol L^{-1} $(NH_4)_2SO_4$, 300 mmol L^{-1} sucrose, 3 mmol L^{-1} $MgCl_2$, 1.2 mmol L^{-1} PMSF, 0.5% TritonX-100) at 4 °C for 3 min. The extracted cells were then rinsed in nonenzyme digestion solution (same as extraction solution except with 50 mM NaCl instead of 250 mmol L^{-1} $(NH_4)_2SO_4$), and digested in digestion solution containing DNase I (400 mg L^{-1}) and RNase A (400 mg L^{-1}) for 20 min at 23 °C. After that, the extracted samples were placed in high-ionic strength extraction solution at 23 for 5 min. So far only the nuclear matrix intermediate filament structure remained intact.

2.6.1. Sample preparation for the light microscopy

The cells seeded on cover slip strip were selectively extracted. The NM-IF samples were firstly prefixed in 2% glutaraldehyde (made in nonenzyme digestion solution) at 4 °C for 30 min. Then, after being washed with PBS (pH 7.4) they were stained with 0.2% Coomassie Brilliant Blue G-250. Finally, the NM-IF system was observed under light microscope after the following activities were performed on them including washing with water, airing, vitrification with xylene and enveloping with resin.

2.6.2. Sample preparation for the electron microscope

The NM-IF samples on the nickel grids were prefixed in 2% glutaraldehyde (made in nonenzyme digestion solution) at 4 °C for 30 min. They were then washed with PBS (pH 7.4), post-fixed in 1% OSO_4 at 4 °C for 5 min, dehydrated in ethanol series, replaced in isoamyl acetate, and dried through the CO_2 critical point. The NM-IF samples were examined with a JEM-100CX II transmission electron microscope (TEM).

2.7. Immunogold staining sample preparation

The NM-IF samples on the nickel grids were blocked by 5% BSA at 37 °C for 30 min and incubated with NPM primary antibody (1:100) at room temperature for 1–2 h. They were then incubated with 5% BSA for

30 min, washed with PBS (pH 8.2), and incubated with the secondary antibody (1:30) which were labeled with colloidal gold (10–15 nm) for 2 h. After that, they were washed with PBS, incubated with 3% paraformaldehyde and 2% glutaraldehyde for 10 min, post-fixed in 1% OSO_4 at 4 °C for 5 min, dehydrated in ethanol series, replaced in isoamyl acetate, and dried through the CO_2 critical point. At last, the immunogold staining samples were observed under TEM.

2.8. Sample preparation for the fluorescence microscopy

The NM-IF samples on the cover slip strip were prefixed in 4% paraformaldehyde at 4 °C for 10 min, blocked by 5% BSA at room temperature for 1 h, incubated with NPM primary antibody (1:300) and then with secondary antibody (1:1000) which was labeled with fluorescence dye Cy3 (red), washed with water and dried by airing. After that, they were enveloped with 90% glycerol and then observed under fluorescence microscopy. The whole process after incubation with secondary antibody should be performed in the dark.

2.9. Sample preparation for LSCM

The cells on the cover slip strip were submerged in PBS or TBS (including 0.5% Triton X-100) at 37 °C for 30 min. After being washed with PBS, the cells were fixed in 4% paraformaldehyde for 10 min, blocked by 5% BSA at room temperature for 1 h, and then incubated with dual primary antibodies at room temperature for 30 min and then 4 °C overnight. The dual primary antibody sets comprised of NPM/c-fos, NPM/c-myc, NPM/Rb and NPM/P53.

After being washed with TTBS thrice for 30 min, the cells were incubated with different secondary antibodies sets which were labeled with Cy3 or FITC (green), washed with TTBS for 4× 10 min and with water for 2× 5 min, enveloped with 90% glycerol after airing and then observed under LSCM.

3. Results

3.1. Results of 2D PAGE and image analysis

The nuclear matrix proteins extracted from MG-63 cells and the cells treated with RCT were subjected to 2D PAGE (Fig. 1A). Quantificational analysis of image for three repeat sets silver-stained 2D gels was performed using PDQuest 8.0 software (Bio-Rad).

3.2. Results of MALDI-TOF-MS analysis and database search

After MALDI-TOF-MS analysis and Swiss-Prot database search, two protein spots (Fig. 1B and C) with altered expression are identified as nucleophosmin (Table 1).

3.3. Western blot of nucleophosmin

The nucleophosmin immunoband with a molecular weight of 38 kDa was observed in both NM-IF samples of control and RCT-treated cells. The immunoband of control cells is wider and thicker than that of RCT-treated cells. The intensity of the band of NPM protein changed 13.87-fold. It indicates the down-regulated expression of nucleophosmin after RCT treatment which is consistent with the results of 2D PAGE analysis (Fig. 2).

3.4. The localization and expression of nucleophosmin in the nuclear matrix of MG-63 cells

3.4.1. Results of light microscopy

Light microscopy observation revealed that the intermediate filaments in MG-63 were not well distributed and the amount of which was rather small. Lamina, which was thick and uneven, was deeply stained. The nuclear matrix filaments in MG-63 cells were not well distributed and they were arranged irregularly. More residual nucleoli were usually observed within the nucleus region (Plate I, 1). However, in the MG-63 cells induced by RCT, the karyoplasmic ratio decreased, the whole framework outspread to a greater extent, and the NM-IF system showed characteristics of uniform distribution. The intermediate filaments, dyed uniformly, spread from the region around nucleus to the cellular edge and formed a well-distributed and regular network throughout the cytoplasm region. Lamina became thinner. The nuclear matrix filaments were abundant and well distributed (Plate I, 2).

The localization and expression of nucleophosmin was revealed after observing the immunofluorescence. The results showed that the highly intensified NPM immunofluorescence mainly distributed in the residual nucleoli region of MG-63 cells, and the intensity of fluorescence was very low in the nuclear matrix and lamina regions (Plate I, 3). After treatment by RCT, the distribution of NPM changed evidently. The intensity of immunofluorescence within the nucleus region dropped, especially in the nucleoli region while that in the lamina

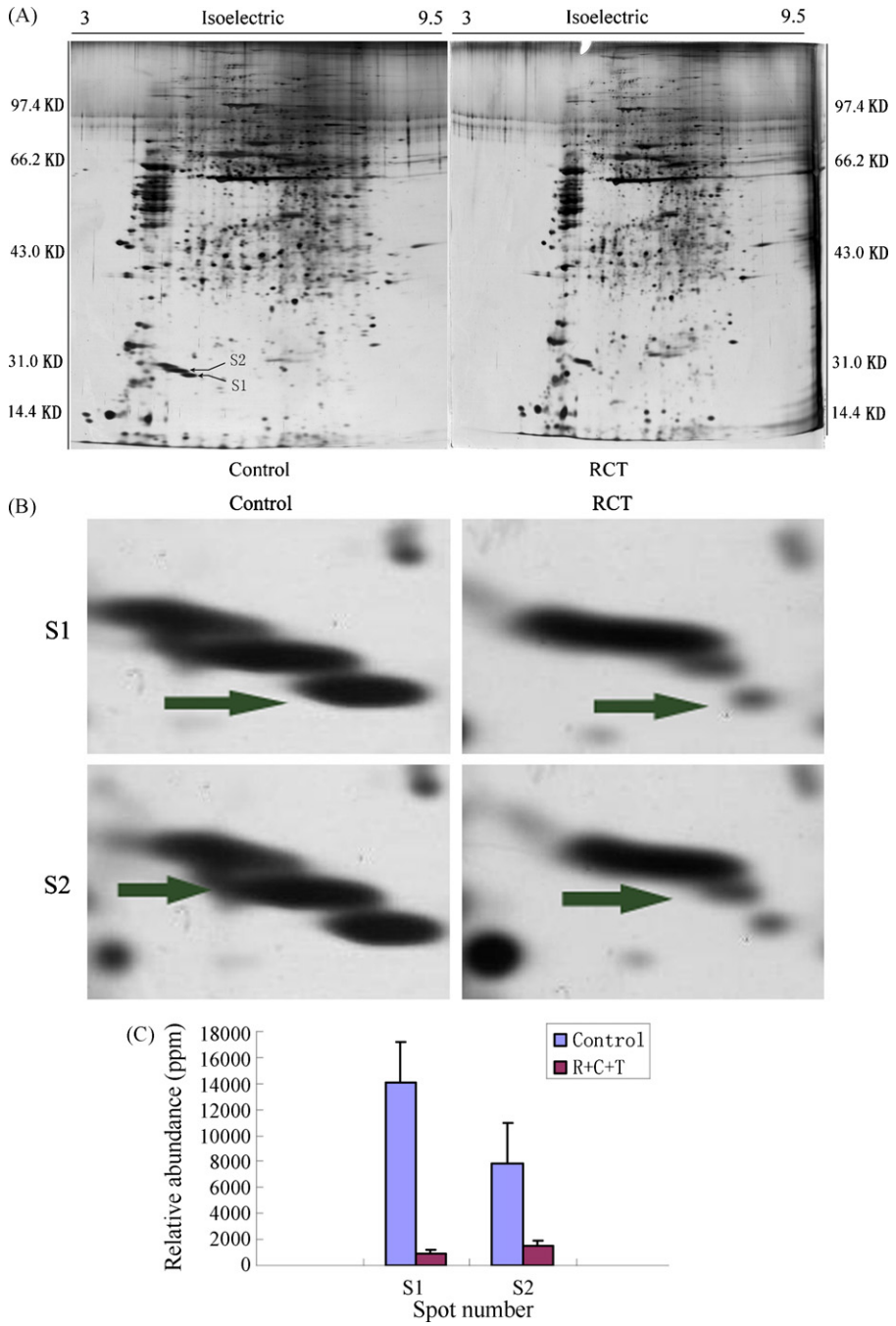

Fig. 1. 2D protein profiles from nuclear matrix of human osteosarcoma MG-63 cells. Proteins were separated on the basis of pI (*X*-axis) and molecular mass (*Y*-axis) and visualized by silver staining. The proteins were identified by MALDI-TOF-MS, and nucleophosmin proteins are shown as symbols on the gels. (A) 2-DE pattern from nuclear matrix of MG-63 cells. Labeled spots S1 and S2 indicated down-regulated nucleophosmin proteins. (B) Enlarged portions of nucleophosmin protein spots from 2-DE gels. Arrows indicate nucleophosmin protein spots. (C) Optical density changes of identified nucleophosmin protein spots.

and karyotheca regions ascended. NPM also displayed the tendency of transferring from nucleoli regions to nuclear matrix. Faint fluorescence could be observed even in the intermediate filaments (Plate I, 4).

3.4.2. Results of the transmission electron microscope

The observation showed that the framework of nuclear matrix, lamina and intermediate filaments joined

Table 1
The nuclear matrix proteins identified as nucleophosmin by MS

Spot ID.	Protein names	Swiss-Prot ID	Theoretic Mr	pI	Score/coverage	Peptides matched
S1	Nucleophosmin	P06748	32,726	4.64	58/28%	6
S2	Nucleophosmin	P06748	32,726	4.64	64/28%	6

each other and formed an interlinking and integrated NM-IF network system. In the NM-IF system of MG-63 cell, the filaments were relatively few and scattered. They were not well distributed and arranged irregularly. The nuclear lamina in MG-63 cells was ununiformly thick and compact. The inner nuclear lamina was connected to some thick nuclear matrix filament bundles, and the outer nuclear lamina was connected to some thin and short intermediate filaments. The intermediate filaments which were not big in number were chiefly thick bundles with only a few single filaments. They were distributed unevenly and arranged irregularly (Plate I, 5).

In MG-63 cells treated with RCT, in which the single filaments increased, the nuclear matrix filaments were abundant, slender and well distributed. The nuclear lamina in induced cells turned into a thin and uniform fibroid structure. Quite a few single filaments were found in intermediate filaments which interweaved with the slender intermediate filament bundles into a well distributed and regular network throughout the cytoplasm region. The nuclear matrix, lamina and intermediate filaments connected closely to each other, and formed a compact and regular network. The configuration of NM-IF system in treated cell displayed typical features of normal cells (Plate I, 6).

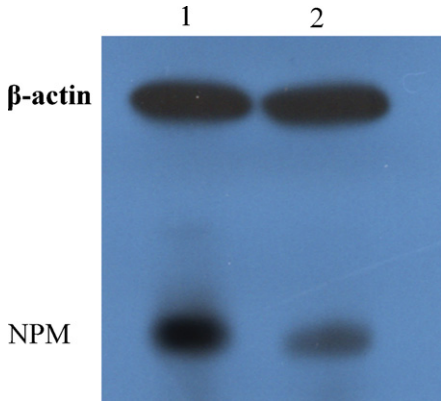

Fig. 2. Confirm of the differential expression of NPM by western blot. The selectively extracted nuclear matrix proteins (15 μg/band) were applied to an SDS-polyacrylamide gel, separated by electrophoresis, and transferred to PVDF membrane by electroblotting. NPM was then detected using anti-NPM mouse monoclonal antibody. β-Actin was also detected as inner control using rabbit monoclonal antibody. Horseradish peroxidase-conjugated goat anti-mouse and anti-rabbit IgG were used as secondary antibody, respectively. The bands were detected by enhanced chemiluminescence (ECL) detection system. Lane 1 is the nuclear matrix proteins sample of MG-63 cells and lane 2 is the sample of RCT treated MG-63 cells.

TEM observation for NPM which was labeled with immunogold revealed that black high-density immunogold granule were found in the nuclear matrix filaments of MG-63 cells (Plate I, 7) and the MG-63 cell treated by RCT (Plate I, 8). This indicated NPM was located in the nuclear matrix filaments system. In MG-63 cells, there were more immunogold granules which distributed fascicularly in the nuclear matrix. But in the MG-63 cells treated by RCT, there were few immunogold granules and they distributed singly or fascicularly.

3.5. The co-localization between NPM and the products of oncogenes, antitumor genes

The cells were dyed with special dual antibody sets which were labeled with different fluorescent dye. The antibody sets comprised of NPM/c-fos, NPM/c-myc, NPM/Rb and NPM/P53. NPM was dyed with cy3 and the opposite proteins in each set were dyed with FITC. The localization of NPM and the opposite proteins were observed with LSCM. The co-localization fluorescence was yellow or orange when two different fluorescence overlapped (Plate II).

3.5.1. The co-localization between NPM and c-fos in MG-63 cells

In MG-63 cells, the highly-intensified red fluorescence of NPM mainly distributed in nucleolus region, and the intensity of fluorescence in cytoplasm was very low (Plate II, 1). The highly intensified fluorescence of c-fos distributed mainly in karyon in clusters and punctate fluorescence could be found in cytoplasm (Plate II, 2). The yellow overlapped fluorescence indicated co-localization between NPM and c-fos especially in nucleolus region (Plate II, 3).

In MG-63 cells treated with RCT, the unitary intensity of NPM fluorescence weakened. NPM fluorescence in nucleolus regions became weak, but the dispersed fluorescence in karyoplasm intensified, which seems to indicate the transference of NPM from nucleolus region

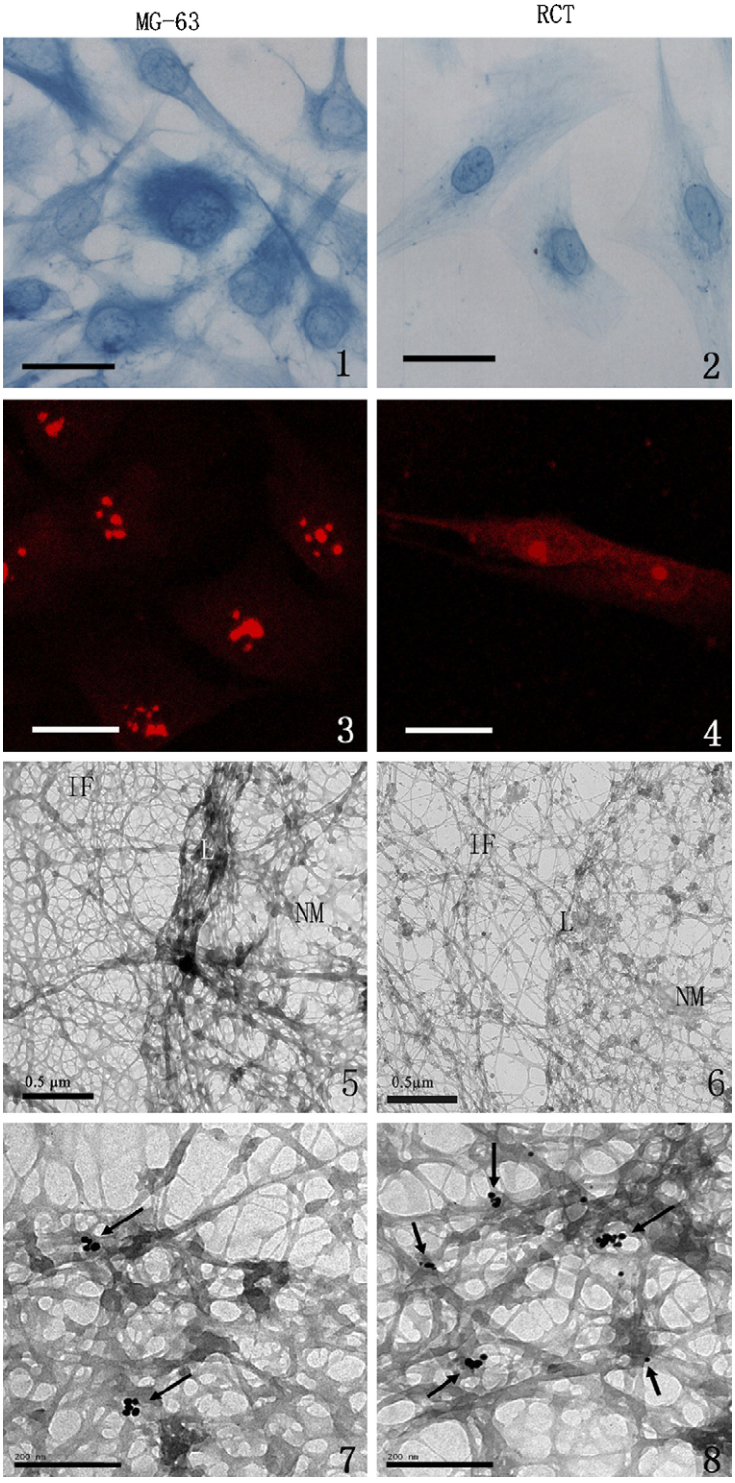

Plate I. (1, 2) Observation of NM-IF system in MG-63 cells (1) and treated cells (2) by light microscopy (dyed by CBB G-250, bar = 30 μm); (3, 4) distribution of NPM in the NM-IF system of MG-63 (3) and treated cells (4) cells by fluorescence microscopy (labeled with fluorescence dye CY3, bar = 30 μm); (5, 6) observation of NM-IF system in MG-63 cells (5) and treated cells (6) by TEM (NM = nuclear matrix, L = lamina, IF = intermediate filaments, bar = 0.5 μm); (7, 8) distribution of NPM in the NM-IF system of MG-63 cells (7) and treated cells (8) by TEM (labeled with immunogold granule, bar = 200nm).

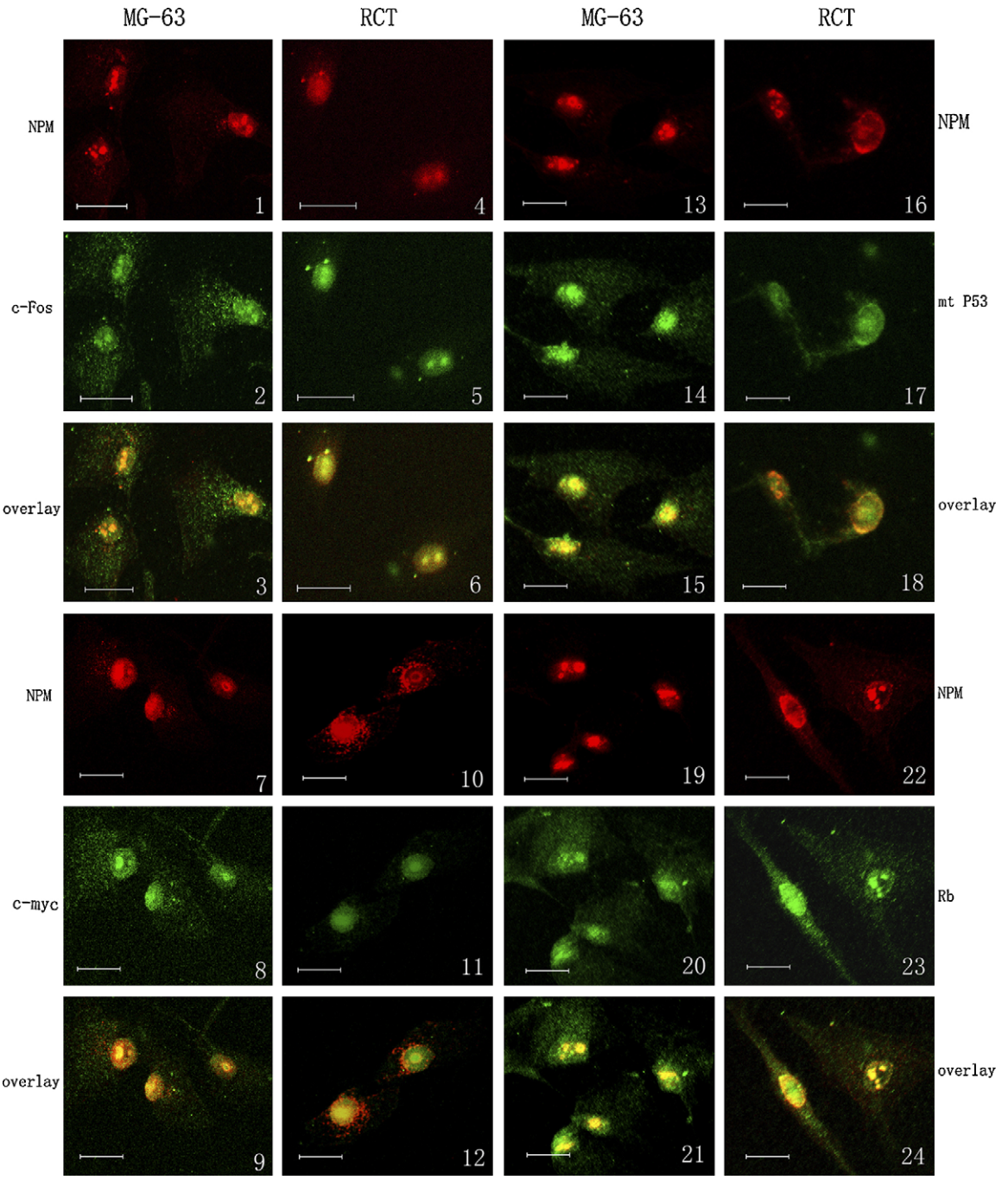

Plate II. (1–6) Expression of NPM and c-fos in MG-63 cells. The overlay indicated the co-localization relationship between NPM and C-fos (bar = 30 μm); (7–12) expression of NPM and c-myc in MG-63 cells. The overlay indicated the co-localization relationship between NPM and P53 (bar = 30 μm); (13–18) expression of NPM and mtP53 in MG-63 cells. The overlay indicated the co-localization relationship between NPM and C-myc (bar = 30 μm); (19–24) expression of NPM and Rb in MG-63 cells. The overlay indicated the co-localization relationship between NPM and RB (bar = 30 μm).

to karyoplasm (Plate II, 4). It could also be observed that the unitary intensity of c-fos fluorescence weakened. C-fos fluorescence clustered in nucleolus regions and dispersed in cytoplasm (Plate II, 5). There was still overlap of fluorescence which indicated co-localization between NPM and c-fos especially in nucleolus, but the intensity of the co-localized fluorescence weakened (Plate II, 6).

3.5.2. The co-localization between NPM and c-myc in MG-63 cells

In MG-63 cells, the highly intensified red fluorescence of NPM clustered around nucleolus region and some center of nucleolus became vacuolar. Some faint punctuate fluorescence dispersed in cytoplasm (Plate II, 7). The highly intensified fluorescence particle of c-myc distributed mainly in nucleolus and peripheral regions, and a little dispersed green fluorescence could be found in cytoplasm (Plate II, 8). The overlapped fluorescence indicated there was co-localization in karyon, and the intensity of overlapped fluorescence in nucleoli was the highest (Plate II, 9).

In MG-63 cells induced by RCT, the red fluorescence of NPM could be found both in karyon and cytoplasm. The intensity of fluorescence in karyon became weak and the nucleolus became vacuolar. Strong red fluorescence clustered in cytoplasm and distributed mainly around karyotheca. NPM tended to transfer from nucleolus to karyotheca and cytoplasm (Plate II, 10). The dispersed fluorescence of c-myc, which distributed mainly in nucleolus, became weak. The fluorescence of c-myc in cytoplasm also weakened, or even disappeared (Plate II, 11). The overlapped fluorescence of NPM and c-myc indicated co-localization in nuclear lamina and nucleolus regions, and the co-localized fluorescence in nucleolus became weaker (Plate II, 12).

3.5.3. The co-localization between NPM and mtP53 in MG-63 cells

In MG-63 cells, the highly intensified red fluorescence of NPM which clustered mainly around nucleolus region and dispersed faint fluorescence could be found in karyoplasm (Plate II, 13). The mutant of P53 protein (mtP53) distributed mainly in karyon (the half-life of wild P53 is very short, and the protein that immunofluorescence indicated is mtP53 which has a longer half-life). The highly intensified fluorescence of mtP53 lumped in karyon, and faint fluorescence could be found in cytoplasm (Plate II, 14). The overlapped fluorescence of NPM and mtP53 indicated co-localization in nucleolus regions (Plate II, 15).

In MG-63 cells induced by RCT, the fluorescence of NPM weakened in karyon, but increased in nuclear lamina and inner regions (Plate II, 16). This suggested the transference of NPM from nucleolus to karyoplasm and nuclear lamina. After treatment, the whole green fluorescence of mtP53 weakened, and the fluorescence in inner karyotheca increased markedly (Plate II, 17). The overlapped fluorescence indicated the co-localization in nucleolus and nuclear lamina between NPM and mtP53 after treatment (Plate II, 18).

3.5.4. The co-localization between NPM and Rb in MG-63 cells

In MG-63 cells, NPM clustered mainly around nucleolus region and the intensity of fluorescence was high (Plate II, 19). Most Rb distributed unevenly in the nucleus, and the intensity of fluorescence was faint in cytoplasm (Plate II, 20). The overlapped fluorescence indicated that they had co-localization nucleolus regions (Plate II, 21). After treatment with RCT, the distribution of NPM changed in induced cells. The fluorescence of NPM increased in nuclear lamina but decreased in nucleolus regions (Plate II, 22). It indicated that the fluorescence tended to transfer from nucleolus to karyoplasm and karyotheca. Faint fluorescence of NPM could be found in cytoplasm. The intensity of Rb fluorescence increased markedly after treatment with RCT. Rb congregated mainly in the nucleus and karyotheca in induced cells. In some treated cells, dispersed Rb fluorescence could be found in karyon (Plate II, 23). The overlapped fluorescence indicated the co-localization in nucleolus and nuclear lamina between NPM and Rb after treatment, and the co-localization fluorescence transferred from nucleolus to nuclear lamina (Plate II, 24).

4. Discussion

4.1. The changes of expression and localization of nucleophosmin in the nuclear matrix

NPM distributes mostly in the nucleolus granule regions and can shuttle between karyon and cytoplasm. There were only a few reports about its localization in nuclear matrix. Previous studies (Subong et al., 1999; Yun et al., 2003) showed that NPM existed in the nuclear matrix of human prostate cancer cells and hepatoma cells. The re-localization of NPM was affected by cell cycle phase and some cytotoxin (Chou & Yung, 1995). The changes of localization and expression of NPM play an important role in the regulation of cell differentiation.

In this study, the results of 2D quantitative analysis, mass spectrum and western blot revealed that NPM existed in the sample of nuclear matrix and the expression of NPM in nuclear matrix decreased markedly after treatment with RCT. NPM was found to locate in the nuclear matrix filament system via immunogold transmission electron microscopy. It was also observed in the nucleus of karyotheca and cytoplasm via immunofluorescence microscopy and LSCM after RCT-induction of MG-63 cells. After RCT treatment, NPM translocated from nucleolus to nucleoplasm and cytoplasm while the total level of NPM in the cell did not change significantly in control and RCT-treated MG-63 cells. The

soluble NPM in cytoplasm was increased as demonstrated in immunocytochemistry. The most prominent change was NPM reduction in association with nuclear matrix. This indicated that NPM localization in nuclear matrix was directly related to NPM function in differentiation. Although immunogold dots could not accurately quantify NPM localization in nucleolus or nucleoplasm, it served a rough estimation of NPM translocation from nucleolus to nucleoplasm. We think the structural changes of nuclear matrix after RCT induction might be directly associated with NPM translocation.

What is more, previous researches had found the overexpression of NPM were in many tumor cells and the down-regulated expression in the differential cells induced by retinoic acid (Alsayed et al., 2001). They were in accordance with our study in which the expression of NPM was down-regulated during the differentiation induced by the combination of effective composition of Chinese herbs and drugs (RCT). This indicated that NPM was an important regulator during the modulation of cell canceration and reversion.

The results of immunofluorescence microscopy and LSCM confirmed qualitatively the down-regulated expression of NPM in nuclear matrix. Some researchers reported the cell cycle phase-dependent changes of localization of NPM, and the translocation from nucleolus to karyoplasm after being treated with cytotoxin drugs (Chan & Chan, 1999). However, there was not any report about the localization changes of NPM in the nuclear matrix of tumor cells during the induced differentiation, and we do not know the mechanism of the translocation. As a multifunctional nuclear matrix protein, the re-localization of NPM might serve as a mechanism of modulation, which participates in the regulation during the cell differentiation induced by RCT, which deserves further study. The results of our study confirmed that NPM was a nuclear matrix protein located in the nuclear matrix filaments, and the expression and localization of NPM in nuclear matrix changed markedly during the induced differentiation. Further research for the alteration of the expression and localization of NPM will contribute to the elucidation of the effect of NPM in the induced differentiation of MG-63 cells.

4.2. The co-localizational relationship between NPM and the products of correlative genes and its alteration

Being an important regulator and chaperone, NPM participates in the modulation of cell differentiation through its interaction with many correlative products of oncogenes and antitumor genes.

The results of LSCM showed that there were similar co-localization relationship between NPM and the products of oncogenes c-fos, c-myc, and tumor suppressor genes Rb, P53 in MG-63 cells, respectively. After the treatment with RCT, the co-localizative immunofluorescence weakened and transferred from nucleolus to karyoplasm and karyotheca. Meanwhile, the results of LSCM qualitative analysis revealed the up-regulative expression of RB gene and the down-regulative expression of gene c-fos, c-myc and mtP53. Immunocytochemistry gives rise of indirect co-localization of NPM and other cancer related genes. NPM also serves as chaperone function and potential interactions of NPM with other oncogenes and tumor suppressor genes are important. We plan to further investigate this possibility. Co-localization of c-myc and c-fos with NPM does not mean direct association that requires biochemical evidence. Subcellular localization of c-myc and c-fos could change in different cell lines and we observed more concentrated immunofluorecense in the nucleolus of MG-63 cells might represent more active nucleolus in cancer cells.

The activation of c-myc could make cells to enter S phase and complete the replication of DNA, and the overexpression of c-myc could accelerate the proliferation of cells. The dimeric transcription factor Ap-1, which is composed of c-fos and c-Jun, participates in the cell regulation of growth, development and differentiation. Nucleophosmin was identified as a candidate myc-responsive gene and the NPM peptide sequence was bound by c-myc in vivo (Zeller et al., 2001). The increasing expression of c-myc gene will improve the level of NPM transcription (Guo et al., 2000). NPM co-localized with c-myc and c-fos, respectively in nucleus and the co-localization altered after the induced differentiation of cells. This indicated that the products of these genes might have direct interaction and the interaction could be a new mechanism for cell differentiation. However, there has not been any report about the co-localizational relationship.

Previous researches revealed that NPM could integrate with NF-κb (Dhar, Lynn, Daosukho, & St Clair, 2004) and phosphorylated pRb (Lin, Liang, & Yung, 2006), influence the gene transcription through the alteration of E2F1 expression, and accelerate the running of cell cycle. The down-regulated expression of NPM protein could block cell cycle. And low-phosphorylated pRb could restrain the activation of transcription mediated by E2F1 and block the cell cycle in G1 phase. These results displayed that the overexpression of NPM could impel cells into proliferation while the increasing expression of pRb could conduce to block cell cycle in G1 phase

and therefore promote the differentiation of cells. In this study, the treatment of MG-63 cells with RCT decreased the expression of NPM and increased the expression of Rb. These results suggested that RCT blocked the cycle of MG-63 cells by the alterative expression of NPM and Rb. The enhanced co-localizative fluorescence of NPM and Rb in the nuclear lamina during the induced differentiation suggested the enrichment of pRb in the inner region of karyotheca in which the expression of gene was active, and the enrichment of pRb restrained the activation of E2F1. But the mechanism of enrichment has not been reported so far.

The half-life of wild type P53 protein is very short (just about 6 min), so in this study the P53 protein, which was observed by immunocytochemistry, is considered as mutative products of P53 gene whose half-life is longer. Previous researches discovered that the domain at the C-terminus of NPM could interact with two domains of P53, which suggested that they could interact directly, and the interaction could regulate the stability and transcriptional activity of P53 (Colombo et al., 2002; Kurki et al., 2004; Lambert & Buckle, 2006). Previous researches also discovered that NPM participated in the regulation of ARF–P53 tumor suppression pathway (Bertwistle, Sugimoto, & Sherr, 2004). NPM could inhibit the tumor suppressive function of ARF by recruiting ARF to nucleoli (Korgaonkar et al., 2005). Our experiment suggested the co-localization relationship between NPM and P53 and confirmed former research results that NPM interacted with P53 directly. During the differentiation of MG-63 cells, the expression of NPM and mutative products of P53 gene decreased markedly. These results suggested that the reduced expression of NPM made mutative P53 unstable and degraded, and the expression of wild products of P53 gene, which had been restrained, began to increase. This process, in turn, triggered the reversion of tumor cells malignant phenotype. However, we do not understand the biological significance of translocation of the co-localized NPM and P53 during the cell differentiation, which was induced by RCT. It requires further investigation.

The results of our research indicated that NPM interacted respectively, with the products of c-fos, c-myc, mtP53, and Rb gene in karyon, and the locality of interaction altered after the treatment by RCT. It is the first time that the co-localizational relationships among NPM and c-fos, c-myc were found. This provides important scientific base for the mechanism research of MG-63 cell differentiation induced by the combination of Chinese medicine efficacious ingredients. We emphasize NPM in this study because NPM has multiple cellular functions associated with tumor promotion as well as tumor suppressor depending on binding partners, cellular location, and cell cycle. NPM haploinsufficiency that causes cancer vulnerability indicates that it is one of master switches of cancer related genes. RTC anticancer effects might have multiple targets as demonstrated by changes of oncogenes and tumor suppressor genes in our study. The possibility of chaperone function of NPM in relationship of other cancer related genes would be explored in the future study.

All in all, our research found that during the differentiation of MG-63 cells induced by the combination of Chinese medicine efficacious ingredients, NPM localized in nuclear matrix, and altered markedly in localization and expression. It also confirmed that NPM co-localized with c-fos, c-myc, P53, and Rb respectively, and the co-localization altered after the treatment. Such results suggested that the combination of Chinese medicine efficacious ingredients (RCT) regulated the expression and localization of NPM and relative genes in nuclear matrix, blocked cell cycle, and facilitated the terminal differentiation of MG-63 cells. Therefore, we can confidently conclude that NPM played a very important role in the procedure of differentiation though many mechanisms have not been investigated because this procedure involves such a complicated regulative network of NPM and many other regulators. Further researches on the alterations of NPM expression and localization in nuclear matrix and its mechanism in the modulation of tumor cell differentiation will be very significant in the more insightful understanding of the anti-tumor mechanism of Chinese medicine efficacious ingredients and the induced differentiation mechanism of tumor cells.

Acknowledgement

Supported by the National Natural Science Foundation of China, No. 30470877.

References

Alsayed, Y., Uddin, S., Mahmud, N., Lekmine, F., Kalvakolanu, D. V., Minucci, S., et al. (2001). Activation of Rac1 and the p38 mitogen-activated protein kinase pathway in response to all-*trans*-retinoic acid. *Journal of Biological Chemistry*, *276*, 4012–4019.

Bertwistle, D., Sugimoto, M., & Sherr, C. J. (2004). Physical and functional interactions of the Arf tumor suppressor protein with nucleophosmin/B23. *Molecular and Cellular Biology*, *24*, 985–996.

Capco, D. G., Wan, K. M., & Penman, S. (1982). The nuclear matrix: Three-dimensional architecture and protein composition. *Cell*, *29*, 847–858.

Chan, P. K., & Chan, F. Y. (1999). A study of correlation between NPM-translocation and apoptosis in cells induced by daunomycin. *Biochemical Pharmacology*, *57*, 1265–1273.

Chan, P. K., Qi, Y., Amley, J., & Koller, C. A. (1996). Quantitation of the nucleophosmin/B23-translocation using imaging analysis. *Cancer Letters*, *100*, 191–197.

Chou, Y. H., & Yung, B. Y. (1995). Cell cycle phase-dependent changes of localization and oligomerization states of nucleophosmin/B23. *Biochemical and Biophysical Research Communications*, *217*, 313–325.

Colombo, E., Marine, J. C., Danovi, D., Falini, B., & Pelicci, P. G. (2002). Nucleophosmin regulates the stability and transcriptional activity of p53. *Nature Cell Biology*, *4*, 529–533.

Colombo, E., Bonetti, P., Lazzerini Denchi, E., Martinelli, P., Zamponi, R., Marine, J. C., et al. (2005). Nucleophosmin is required for DNA integrity and p19Arf protein stability. *Molecular and Cellular Biology*, *25*, 8874–8886.

Dhar, S. K., Lynn, B. C., Daosukho, C., & St Clair, D. K. (2004). Identification of nucleophosmin as an NF-kappa B co-activator for the induction of the human SOD2 gene. *Journal of Biological Chemistry*, *279*, 28209–28219.

Falini, B., Mecucci, C., Tiacci, E., Alcalay, M., Rosati, R., Pasqualucci, L., et al. (2005). Cytoplasmic nucleophosmin in acute myelogenous leukemia with a normal karyotype. *New England Journal of Medicine*, *352*, 254–266.

Falini, B., Nicoletti, I., Martelli, M. F., & Mecucci, C. (2007). Acute myeloid leukemia carrying cytoplasmic/mutated nucleophosmin (NPMc(+) AML): Biologic and clinical features. *Blood*, *109*, 874–885.

Feuerstein, N., & Mond, J. J. (1987). "Numatrin," a nuclear matrix protein associated with induction of proliferation in B lymphocytes. *Journal of Cellular Biochemistry*, *262*, 11389–11397.

Feuerstein, N., Spiegel, S., & Mond, J. J. (1988). The nuclear matrix protein, numatrin (B23), is associated with growth factor-induced mitogenesis in Swiss 3T3 fibroblasts and with T lymphocyte proliferation stimulated by lectins and anti-T cell antigen receptor antibody. *The Journal of Cell Biology*, *107*, 1629–1642.

Gao, J. G., Han, Y. R., Jiao, R. J., & Zhai, Z. H. (1994). The intermediate filament–lamina–nuclear matrix system of ES-M13 cells. *Shi Yan Sheng Wu Xue Bao*, *27*, 463–475.

Grisendi, S., Bernardi, R., Rossi, M., Cheng, K., Khandker, L., Manova, K., et al. (2005). Role of nucleophosmin in embryonic development and tumorigenesis. *Nature*, *437*, 147–153.

Guo, Q. M., Malek, R. L., Kim, S., Chiao, C., He, M., Ruffy, M., et al. (2000). Identification of c-Myc responsive genes using rat cDNA microarray. *Cancer Research*, *60*, 5922–5928.

Helms, S. (2004). Cancer prevention and therapeutics: *Panax ginseng*. *Alternative Medicine Review*, *9*, 259–274.

Korgaonkar, C., Hagen, J., Tompkins, V., Frazier, A. A., Allamargot, C., Quelle, F. W., et al. (2005). Nucleophosmin (B23) targets ARF to nucleoli and inhibits its function. *Molecular and Cellular Biology*, *25*, 1258–1271.

Kurki, S., Peltonen, K., Latonen, L., Kiviharju, T. M., Ojala, P. M., Meek, D., et al. (2004). Nucleolar protein NPM interacts with HDM2 and protects tumor suppressor protein p53 from HDM2-mediated degradation. *Cancer Cell*, *5*, 465–475.

Lambert, B., & Buckle, M. (2006). Characterisation of the interface between nucleophosmin (NPM) and p53: Potential role in p53 stabilisation. *FEBS Letters*, *580*, 345–350.

Li, J., Zhang, X., Sejas, D. P., & Pang, Q. (2005). Negative regulation of p53 by nucleophosmin antagonizes stress-induced apoptosis in human normal and malignant hematopoietic cells. *Leukemia Research*, *29*, 1415–1423.

Lin, C. Y., Liang, Y. C., & Yung, B. Y. M. (2006). Nucleophosmin/B23 regulates transcriptional activation of E2F1 via modulating the promoter binding of NF-kappa B, E2F1 and pRB. *Cellular Signalling*, *18*, 2041–2048.

Michishita, E., Kurahashi, T., Suzuki, T., Fukuda, M., Fujii, M., Hirano, H., et al. (2002). Changes in nuclear matrix proteins during the senescence-like phenomenon induced by 5-chlorodeoxyuridine in HeLa cells. *Experimental Gerontology*, *37*, 885–890.

Morris, S. W., Kirstein, M. N., Valentine, M. B., Dittmer, K. G., Shapiro, D. N., Saltman, D. L., et al. (1994). Fusion of a kinase gene, ALK, to a nucleolar protein gene, NPM, in non-Hodgkin's lymphoma. *Science*, *263*, 1281–1284.

Nickerson, J. A., Krockmalnic, G., Wan, K. M., & Penman, S. (1997). The nuclear matrix revealed by eluting chromatin from a cross-linked nucleus. *Proceedings of the National Academy of Sciences of the United States of America*, *94*, 4446–4450.

Okuda, M., Horn, H. F., Tarapore, P., Tokuyama, Y., Smulian, A. G., Chan, P. K., et al. (2000). Nucleophosmin/B23 is a target of CDK2/Cyclin E in centrosome duplication. *Cell*, *103*, 127–140.

Okuwaki, M., Matsumoto, K., Tsujimoto, M., & Nagata, K. (2001). Function of nucleophosmin/B23, a nucleolar acidic protein, as a histone chaperone. *FEBS Letters*, *506*, 272–276.

Raimondi, S. C., Dube, I. D., Valentine, M. B., Mirro, J., Jr., Watt, H. J., Larson, R. A., et al. (1989). Clinicopathologic manifestations and breakpoints of the t(3;5) in patients with acute nonlymphocytic leukemia. *Leukemia*, *3*, 42–47.

Redner, R. L. (2002). Variations on a theme: The alternate translocations in APL. *Leukemia*, *16*, 1927–1932.

Savkur, R. S., & Olson, M. O. J. (1998). Preferential cleavage in pre-ribosomal RNA by protein B23 endoribonuclease. *Nucleic Acids Research*, *26*, 4508–4515.

Sparreboom, A., Cox, M. C., Acharya, M. R., & Figg, W. D. (2004). Herbal remedies in the United States: Potential adverse interactions with anticancer agents. *Journal of Clinical Oncology*, *22*, 2489–2503.

Subong, E. N. P., Shue, M. J., Epstein, J. I., Briggman, J. V., Chan, P. K., & Partin, A. W. (1999). Monoclonal antibody to prostate cancer nuclear matrix protein (PRO: 4-216) recognizes nucleophosmin/B23. *Prostate*, *39*, 298–304.

Szebeni, A., & Olson, M. O. (1999). Nucleolar protein B23 has molecular chaperone activities. *Protein Science*, *8*, 905–912.

Tang, J., Niu, J. W., Xu, D., Li, Z. X., Li, Q. F., & Chen, J. A. (2007). Alteration of nuclear matrix-intermediate filament system and differential expression of nuclear matrix proteins during human hepatocarcinoma cell differentiation. *World Journal of Gastroenterology*, *13*, 2791–2797.

Yun, T. K. (2001). *Panax ginseng*—a non-organ-specific cancer preventive? *Lancet Oncology*, *2*, 49–55.

Yun, J. P., Chew, E. C., Liew, C. T., Chan, J. Y. H., Jin, M. L., Ding, M. X., et al. (2003). Nucleophosmin/B23 is a proliferate shuttle protein associated with nuclear matrix. *Journal of Cellular Biochemistry*, *90*, 1140–1148.

Yung, B. Y. (2007). Oncogenic role of nucleophosmin/B23. *Chang Gung Medical Journal*, *30*, 285–293.

Yung, B. Y., Yang, Y. H., & Bor, A. M. (1991). Nucleolar protein B23 translocation after deferoxamine treatment in a human leukemia cell line. *International Journal of Cancer*, *48*, 779–784.

Zeller, K. I., Haggerty, T. J., Barrett, J. F., Guo, Q. B., Wonsey, D. R., & Dang, C. V. (2001). Characterization of nucleophosmin (B23) as a Myc target by scanning chromatin immunoprecipitation. *Journal of Biological Chemistry*, *276*, 48285–48291.